

Adaptive Trajectory Bundle Method for Roll-to-Roll Manufacturing Systems

Jiachen Li, *Student Member, IEEE* and Shihao Li, *Student Member, IEEE* The University of Texas at Austin
{jiachenli, shihaoli01301}@utexas.edu

Abstract—Roll-to-roll (R2R) manufacturing demands precise tension and velocity control under strict operational constraints. Model predictive control requires gradient computation, while sampling-based methods such as MPPI struggle with hard constraint satisfaction. This paper presents an adaptive trajectory bundle method that achieves rigorous constraint handling through derivative-free sequential convex programming. The approach approximates nonlinear dynamics and costs via interpolated sample bundles, with adaptive trust regions and penalty parameters ensuring robust convergence without manual tuning. Simulations on a six-zone R2R system demonstrate tracking accuracy comparable to gradient-based MPC with superior constraint satisfaction over sampling-based alternatives.

Index Terms—Trajectory bundle method, roll-to-roll manufacturing, derivative-free optimization, constrained control, adaptive sequential convex programming

I. INTRODUCTION

Roll-to-roll (R2R) manufacturing processes are essential for high-throughput production of flexible electronics, photovoltaics, functional films, and advanced materials. These systems transport continuous web material through sequential processing zones, where precise tension and velocity regulation are critical to product quality. Excessive tension causes web breakage, while insufficient tension leads to wrinkling and defects. The control challenge is compounded by strong coupling between adjacent zones, time-varying parameters due to changing roll radii, and strict operational constraints on tensions, velocities, and actuator rates.

Traditional control approaches face fundamental limitations. Model Predictive Control (MPC), while capable of handling constraints, requires accurate gradient information and suffers from computational burden in high-dimensional settings. Sampling-based methods like Model Predictive Path Integral (MPPI) control avoid gradient computation but struggle with hard constraint satisfaction. This motivates the need for a framework combining constraint handling with derivative-free optimization.

A. Related Work

Classical R2R control relies on PID, LQR, and MPC variants to regulate web tension and transport speed. Foundational modeling established tension/velocity decoupling strategies [1], while industrial studies refined adaptive PI/PID implementations for operating-point drift [2], [3]. Recent work

emphasizes advanced control methods [4], [5] and physics-consistent tension models [6], [7]. Manufacturing surveys underline the role of monitoring and feedback design in achieving system robustness [8], [9]. Data-driven approaches report robust constrained tension regulation [10] and AI-assisted tension estimation [11], [12], with reviews pointing to hybrid controllers as a promising direction [13].

Despite these advances, classical methods require extensive tuning and provide limited guarantees under coupled nonlinear dynamics. Advanced MPC formulations demand gradient computation and careful initialization, with computational requirements becoming prohibitive for systems with many zones or long prediction horizons.

MPPI control is inherently unconstrained, typically relying on soft-constraint penalties [14], [15]. Methods to enforce hard constraints include CBF-based shields [15], though these can be myopic [16]. Safe-by-construction approaches such as GS-MPPI embed composite CBFs into dynamics [16], while MPPI-DBaS augments states with discrete barrier states [17]. DualGuard-MPPI integrates Hamilton-Jacobi reachability for provable safety [18]. Other approaches improve sample efficiency using learned surrogates (BC-MPPI) [19], specialized samplers [20], [21], or clustering algorithms to address multimodality [14].

While these MPPI variants succeed in robotics, they face limitations for R2R manufacturing. The single-shooting formulation makes long-horizon planning unstable for coupled multi-zone dynamics, and existing constraint mechanisms either provide soft guarantees, require additional filtering layers, or demand specialized model structures.

Recently, the Trajectory Bundle Method (TBM) introduced a derivative-free optimal control paradigm based on sequential convex programming [22]. Instead of Taylor-series approximations, TBM uses interpolated bundles of sampled trajectories to approximate cost, dynamics, and constraint functions.

B. Contributions

This paper develops an adaptive trajectory bundle method for constrained R2R control. The main contributions are:

- 1) We derive the complete mathematical formulation applying TBM to R2R tension-velocity dynamics, including physics-based cost functions, operational constraints, and asymmetric risk handling for over/under-tensioning. The overall workflow of Algorithm 1 is illustrated in Figure 1.
- 2) We introduce adaptive trust region management and penalty scheduling that automatically adjust based on constraint violation metrics, reducing the need for manual tuning.

This paper was produced by the IEEE Publication Technology Group. They are in Piscataway, NJ.

Manuscript received April 19, 2021; revised August 16, 2021.

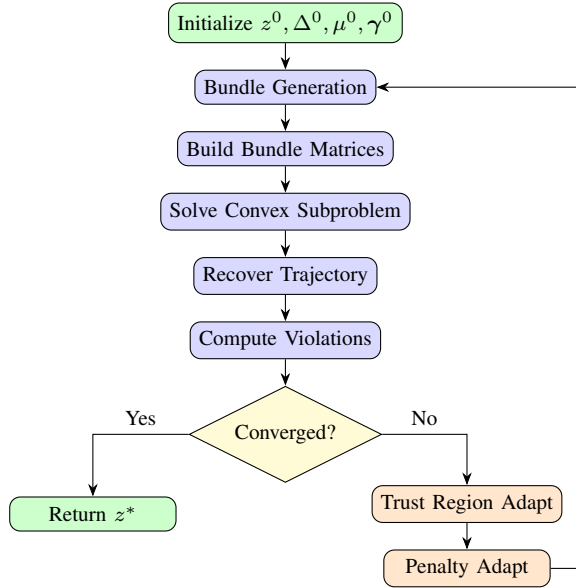


Fig. 1. Flowchart of the Adaptive Trajectory Bundle Method.

3) We establish convergence guarantees for the adaptive TBM, proving that the algorithm achieves feasibility in finite iterations and converges to stationary points of the constrained R2R control problem.

The remainder of this paper is organized as follows. Section II derives R2R system dynamics. Section III presents the adaptive TBM theoretical framework. Section IV establishes convergence guarantees. Section V provides simulation results. Section VI concludes the paper.

II. ROLL-TO-ROLL SYSTEM DYNAMICS

Consider a R2R manufacturing line with N motorized rollers indexed by $i \in \{1, \dots, N\}$, with continuous web material spanning between consecutive rollers. We assume: (1) passive rollers are omitted; (2) web tension T_i is spatially uniform between adjacent rollers; (3) no slippage occurs, giving $v_i = \omega_i R_i$; and (4) the web exhibits linear elastic behavior with Young's modulus E and cross-sectional area A .

The tension dynamics in section i follow from mass conservation:

$$\frac{dT_i}{dt} = \frac{EA}{L_i}(v_i - v_{i-1}) + \frac{1}{L_i}(T_{i-1}v_{i-1} - T_i v_i), \quad (1)$$

where L_i is the span length and boundary conditions $T_0 = T_{N+1} = 0$ apply. The roller velocity dynamics result from torque balance:

$$\frac{dv_i}{dt} = \frac{R_i^2}{J_i}(T_{i+1} - T_i) - \frac{f_i}{J_i}v_i + \frac{R_i}{J_i}u_i + b_i \frac{dw_i}{dt}, \quad (2)$$

where J_i is roller inertia, f_i is viscous friction, u_i is motor torque, and w_i is a Brownian motion capturing stochastic disturbances.

For trajectory optimization, we discretize (1)–(2) using Euler-Maruyama integration with sampling period Δt . Define state $x_t = [T_1, \dots, T_N, v_1, \dots, v_N]^\top \in \mathbb{R}^{2N}$ and control

$u_t = [u_1, \dots, u_N]^\top \in \mathbb{R}^N$. The deterministic propagation map used for bundle construction is:

$$F(x_t, u_t) \triangleq x_t + (f(x_t) + Gu_t)\Delta t, \quad (3)$$

where $f: \mathbb{R}^{2N} \rightarrow \mathbb{R}^{2N}$ encodes the drift terms from (1)–(2) and $G \in \mathbb{R}^{2N \times N}$ maps control inputs to velocity states.

III. ADAPTIVE TRAJECTORY BUNDLE METHOD: THEORETICAL FRAMEWORK

This section develops the adaptive trajectory bundle method for R2R manufacturing control. We first review derivative-free function approximation via trajectory bundles, then formulate the convex subproblem, and finally introduce adaptive mechanisms for trust region and penalty management that eliminate manual tuning.

A. Notation and Preliminaries

Let N denote the number of motorized rollers and H the prediction horizon. The state dimension is $n_x = 2N$ (tensions and velocities) and control dimension is $n_u = N$ (motor torques). A trajectory over horizon H is denoted $z = \{(x_k, u_k)\}_{k=1}^H$ where $x_k \in \mathbb{R}^{n_x}$ and $u_k \in \mathbb{R}^{n_u}$. We endow the trajectory space with the norm:

$$\|z\| = \sqrt{\sum_{k=1}^H (\|x_k\|^2 + \|u_k\|^2)}. \quad (4)$$

The probability simplex is denoted $\Delta^{m-1} = \{\alpha \in \mathbb{R}^m : \sum_{i=1}^m \alpha_i = 1, \alpha_i \geq 0\}$, and $B(z, \Delta) = \{z' : \|z' - z\| \leq \Delta\}$ is the closed ball of radius Δ centered at z . The operator $[\cdot]_- : \mathbb{R}^n \rightarrow \mathbb{R}_{\geq 0}^n$ is defined by $[v]_- = \max(0, -v)$ applied element-wise, extracting the negative part so that $[c]_- > 0$ indicates constraint violation when $c \geq 0$ is required.

B. Derivative-Free Function Approximation via Bundles

The trajectory bundle method approximates nonlinear functions through interpolation of sampled values rather than Taylor series expansion. This approach requires only function evaluations, making it suitable for systems where analytical gradients are expensive or unavailable [23]. The bundle method terminology originates from nonsmooth convex optimization [24], [25], where function values and subgradients are collected into “bundles” to construct piecewise-linear approximations. The trajectory bundle method [22] adapts this philosophy to trajectory optimization using function value interpolation rather than subgradient cutting planes.

1) *Bundle Interpolation:* Consider an arbitrary function $p: \mathbb{R}^a \rightarrow \mathbb{R}^b$. Given a reference point $\bar{y} \in \mathbb{R}^a$ and a sampling radius $\Delta > 0$, we collect m evaluation points $\{y_1, \dots, y_m\} \subset B(\bar{y}, \Delta)$ and compute $p_i = p(y_i)$ for each sample. These are arranged into matrices:

$$W_y = [y_1 \ \dots \ y_m] \in \mathbb{R}^{a \times m}, \quad W_p = [p_1 \ \dots \ p_m] \in \mathbb{R}^{b \times m}. \quad (5)$$

The bundle approximation represents candidate solutions as convex combinations of samples [23]:

$$y = W_y \alpha, \quad p(y) \approx W_p \alpha, \quad \alpha \in \Delta^{m-1}. \quad (6)$$

This construction is exact when p is affine. Importantly, restricting α to the simplex automatically confines solutions to $\text{conv}(\{y_1, \dots, y_m\}) \subseteq B(\bar{y}, \Delta)$, providing an implicit trust region.

2) *Multiple-Shooting Trajectory Representation*: For trajectory optimization over horizon H , we employ a multiple-shooting discretization [26], [27], treating states at discrete time points as independent variables linked through dynamics constraints. At each time index $k \in \{1, \dots, H\}$, we sample m candidate state-control pairs around the current iterate (\bar{x}_k, \bar{u}_k) and evaluate:

$$W_x^{(k)} = \begin{bmatrix} x_1^{(k)} & \dots & x_m^{(k)} \end{bmatrix} \in \mathbb{R}^{n_x \times m}, \quad (7)$$

$$W_u^{(k)} = \begin{bmatrix} u_1^{(k)} & \dots & u_m^{(k)} \end{bmatrix} \in \mathbb{R}^{n_u \times m}, \quad (8)$$

$$W_f^{(k)} = \begin{bmatrix} F(x_1^{(k)}, u_1^{(k)}) & \dots & F(x_m^{(k)}, u_m^{(k)}) \end{bmatrix} \in \mathbb{R}^{n_x \times m}, \quad (9)$$

$$W_r^{(k)} = \begin{bmatrix} r_k(x_1^{(k)}, u_1^{(k)}) & \dots & r_k(x_m^{(k)}, u_m^{(k)}) \end{bmatrix} \in \mathbb{R}^{n_r \times m}, \quad (10)$$

$$W_c^{(k)} = \begin{bmatrix} c_k(x_1^{(k)}, u_1^{(k)}) & \dots & c_k(x_m^{(k)}, u_m^{(k)}) \end{bmatrix} \in \mathbb{R}^{n_c \times m}, \quad (11)$$

where F is the discrete-time dynamics map (3), r_k is the stage cost residual, and c_k captures operational constraints at step k . Here $c_k = (c_{\text{hard},k}, c_{1,k}, \dots, c_{J,k})$ decomposes into hard constraints (state/input bounds) and J classes of soft constraints. We denote the corresponding bundle matrices as $W_{c,\text{hard}}^{(k)}$ and $W_{c,j}^{(k)}$ for $j = 1, \dots, J$.

C. Constrained Bundle Subproblem

Using the bundle matrices, we formulate a convex approximation of the nonlinear trajectory optimization problem. At iteration ℓ , the subproblem is:

$$\begin{aligned} & \underset{\alpha, s, w, d}{\text{minimize}} && \sum_{k=1}^H \|W_r^{(k)} \alpha^{(k)}\|_2^2 + \mu_\ell \sum_{k=1}^{H-1} (\|s_k\|_1 + \|w_k\|_1) \\ & && + \sum_{j=1}^J \gamma_{j,\ell} \sum_{k=1}^{H-1} \|d_{k,j}\|_1 \\ & \text{subject to} && W_f^{(k)} \alpha^{(k)} = W_x^{(k+1)} \alpha^{(k+1)} + s_k, \\ & && W_{c,h}^{(k)} \alpha^{(k)} + w_k \geq 0, \\ & && W_{c,j}^{(k)} \alpha^{(k)} + d_{k,j} \geq 0, \quad j = 1, \dots, J, \\ & && \alpha^{(k)} \in \Delta^{m-1}, \quad k = 1, \dots, H, \\ & && s_k \in \mathbb{R}^{n_x}, w_k \geq 0, d_{k,j} \geq 0, \end{aligned} \quad (12)$$

where $s_k \in \mathbb{R}^{n_x}$ are slack variables for dynamics defects (unconstrained in sign), $w_k \in \mathbb{R}_{\geq 0}^{n_{\text{hard}}}$ are non-negative slack variables for hard inequality constraints (state/input bounds), and $d_{k,j} \in \mathbb{R}_{\geq 0}^{n_j}$ are non-negative slack variables for soft constraint class $j \in \{1, \dots, J\}$. The penalty parameter $\mu_\ell > 0$ penalizes dynamics and hard constraint violations, while $\gamma_{j,\ell} > 0$ penalizes soft constraint violations in class j . The use of ℓ_1 norms for exact penalty functions follows classical approaches in constrained optimization [28], [29].

Problem (12) is a convex optimization problem: the objective combines a convex quadratic term with convex ℓ_1

penalties, all constraints are linear, and the feasible region is a Cartesian product of simplices and non-negative orthants.

After solving (12), the candidate trajectory is recovered via:

$$x_k^{\ell+1} = W_x^{(k)} \alpha^{(k)*}, \quad u_k^{\ell+1} = W_u^{(k)} \alpha^{(k)*}, \quad k = 1, \dots, H. \quad (13)$$

Remark 1 (Relationship to Original TBM). *The formulation (12) extends the original trajectory bundle method [22] in two key aspects:*

(i) **Multiple Penalty Classes**: *The original TBM uses a single penalty parameter μ for all constraints. We introduce constraint classes indexed by $j \in \{1, \dots, J\}$ with separate penalties γ_j , enabling asymmetric treatment of different violation types. For R2R systems, this is critical for safety: over-tension (web breakage risk) is penalized more heavily ($\gamma_+ = 100$) than under-tension (wrinkling, $\gamma_- = 10$).*

(ii) **Adaptive Penalty Scheduling**: *While the original TBM uses fixed penalties, we allow μ_ℓ and $\gamma_{j,\ell}$ to adapt based on observed constraint violations, eliminating the need for manual penalty tuning (see Section III-D below).*

D. Adaptive Mechanisms

The original TBM [22] uses fixed penalty parameters throughout optimization. While effective, this requires manual tuning and lacks convergence guarantees. We introduce adaptive mechanisms for trust region and penalty management that automatically adjust based on constraint satisfaction metrics. Classical trust region methods adapt Δ based on the ratio of actual to predicted objective reduction [30]. Our adaptation rules instead use constraint violation metrics, following the philosophy of [22] while introducing separate penalty classes for asymmetric constraint treatment.

1) *Constraint Violation Metrics*: We define separate violation metrics for each constraint type:

Definition 1 (Constraint Violation Metrics). *Given optimal slack variables $(s^*, w^*, \{d_j^*\})$ from subproblem (12) at iteration ℓ :*

$$\nu_{\text{dyn}}^\ell = \max_{k=1, \dots, H-1} \|s_k^*\|_\infty, \quad (14)$$

$$\nu_{\text{hard}}^\ell = \max_{k=1, \dots, H-1} \|w_k^*\|_\infty, \quad (15)$$

$$\nu_j^\ell = \sum_{k=1}^{H-1} \|d_{k,j}^*\|_1, \quad j = 1, \dots, J. \quad (16)$$

2) *Trust Region Adaptation*: The trust region radius $\Delta^\ell > 0$ controls the locality of the bundle approximation. We adapt it based on constraint satisfaction:

$$\Delta^{\ell+1} = \begin{cases} \min(\beta_{\text{exp}} \Delta^\ell, \Delta_{\text{max}}) & \text{if } \nu_{\text{dyn}}^\ell < \tau_{\text{feas}} \text{ and } \nu_{\text{hard}}^\ell < \tau_{\text{feas}}, \\ \max(\beta_{\text{con}} \Delta^\ell, \Delta_{\text{min}}) & \text{if } \nu_{\text{dyn}}^\ell > \tau_{\text{viol}} \text{ or } \nu_{\text{hard}}^\ell > \tau_{\text{viol}}, \\ \Delta^\ell & \text{otherwise,} \end{cases} \quad (17)$$

where $\beta_{\text{exp}} > 1$ is the expansion factor, $\beta_{\text{con}} < 1$ is the contraction factor, and $\Delta_{\text{min}}, \Delta_{\text{max}}$ bound the trust region radius. The thresholds satisfy $0 < \epsilon_{\text{feas}} < \tau_{\text{feas}} < \tau_{\text{viol}}$, where

Algorithm 1 Adaptive Trajectory Bundle Method

Require: Initial trajectory $z^0 = \{(x_k^0, u_k^0)\}_{k=1}^H$, parameters $(\Delta^0, \mu^0, \gamma^0)$

Ensure: Converged trajectory z^*

- 1: $\ell \leftarrow 0$
- 2: **while** not converged **do**
- 3: **Sample:** Generate $\mathcal{Y}^\ell = \{y_1, \dots, y_m\} \subset B(z^\ell, \Delta^\ell)$ with $z^\ell \in \mathcal{Y}^\ell$
- 4: **Build Bundles:** Evaluate $W_x^{(k)}, W_u^{(k)}, W_f^{(k)}, W_r^{(k)}, W_c^{(k)}$ for $k = 1, \dots, H$
- 5: **Solve Subproblem:** Compute $(\alpha^*, s^*, w^*, \{d_j^*\})$ from (12)
- 6: **Recover Trajectory:** $z^{\ell+1} \leftarrow \{(W_x^{(k)} \alpha^{(k)*}, W_u^{(k)} \alpha^{(k)*})\}_{k=1}^H$
- 7: **Compute Violations:** $\nu_{\text{dyn}}^\ell \leftarrow \max_k \|s_k^*\|_\infty$, $\nu_{\text{hard}}^\ell \leftarrow \max_k \|w_k^*\|_\infty$, $\nu_j^\ell \leftarrow \sum_k \|d_{k,j}^*\|_1$
- 8: **Adapt Trust Region:** Update $\Delta^{\ell+1}$ via (17)
- 9: **Adapt Penalties:** Update $\mu^{\ell+1}$ via (18) and $\gamma_j^{\ell+1}$ via (19)
- 10: **Check Convergence:** If $\nu_{\text{dyn}}^\ell < \epsilon_{\text{feas}}$ and $\nu_{\text{hard}}^\ell < \epsilon_{\text{feas}}$ and $\|z^{\ell+1} - z^\ell\| < \epsilon_z$: **break**
- 11: $\ell \leftarrow \ell + 1$
- 12: **end while**
- 13: **return** $z^{\ell+1}$

ϵ_{feas} is the convergence tolerance, τ_{feas} triggers trust region expansion, and τ_{viol} triggers contraction and penalty increase.

The rationale is as follows: when violations are small (below τ_{feas}), the bundle approximation is accurate over a larger region, justifying trust region expansion; when violations are large (above τ_{viol}), the approximation is poor, so reducing Δ forces samples closer to z^ℓ for better local accuracy; when violations are moderate (between τ_{feas} and τ_{viol}), the current sampling is appropriate and the trust region radius is maintained.

3) *Penalty Adaptation:* Penalty parameters increase when violations persist above thresholds. This finite stabilization property is standard for geometrically increasing penalty sequences [31]. Since μ penalizes both dynamics and hard constraint violations in the subproblem (12), we increase μ when either type of violation exceeds its threshold:

$$\mu^{\ell+1} = \begin{cases} \min(\rho_\mu \mu^\ell, \mu_{\text{max}}) & \text{if } \nu_{\text{dyn}}^\ell > \tau_{\text{viol}} \text{ or } \nu_{\text{hard}}^\ell > \tau_{\text{viol}}, \\ \mu^\ell & \text{otherwise.} \end{cases} \quad (18)$$

Similarly, soft constraint penalties increase when their respective violations exceed thresholds:

$$\gamma_j^{\ell+1} = \begin{cases} \min(\rho_\gamma \gamma_j^\ell, \gamma_{j,\text{max}}) & \text{if } \nu_j^\ell > \tau_j, \\ \gamma_j^\ell & \text{otherwise,} \end{cases} \quad j = 1, \dots, J, \quad (19)$$

where $\rho_\mu, \rho_\gamma > 1$ are increase factors, and $\tau_{\text{viol}}, \tau_j$ are violation thresholds.

Algorithm 1 provides the complete specification.

IV. CONVERGENCE ANALYSIS

This section establishes convergence guarantees for Algorithm 1. We prove that the adaptive mechanisms drive constraint violations to zero and the algorithm converges to stationary points of the penalized objective, which coincide with stationary points of the original constrained R2R control problem under sufficient penalty magnitudes. The proof structure follows classical trust region convergence theory [30], adapted to the penalty formulation and always-accept strategy of [22].

We first define the penalized objective function that underlies the convergence analysis.

Definition 2 (Penalized Objective). *For trajectory $z = \{(x_k, u_k)\}_{k=1}^H$ and penalty parameters $(\mu, \gamma) = (\mu, \gamma_1, \dots, \gamma_J)$, define:*

$$\begin{aligned} \phi_{\mu, \gamma}(z) = & \sum_{k=1}^H \|r_k(x_k, u_k)\|_2^2 \\ & + \mu \sum_{k=1}^{H-1} \|x_{k+1} - F(x_k, u_k)\|_1 \\ & + \mu \sum_{k=1}^{H-1} \|[c_{\text{hard}, k}(x_k, u_k)]_-\|_1 \\ & + \sum_{j=1}^J \gamma_j \sum_{k=1}^{H-1} \|[c_{j, k}(x_k, u_k)]_-\|_1, \end{aligned} \quad (20)$$

where $[v]_- = \max(0, -v)$ is applied element-wise, extracting constraint violations.

Assumption 1 (Lipschitz Continuity). *The stage cost residual $r_k : \mathbb{R}^{n_x} \times \mathbb{R}^{n_u} \rightarrow \mathbb{R}^{n_r}$, dynamics map $F : \mathbb{R}^{n_x} \times \mathbb{R}^{n_u} \rightarrow \mathbb{R}^{n_x}$, and constraint functions $c_k : \mathbb{R}^{n_x} \times \mathbb{R}^{n_u} \rightarrow \mathbb{R}^{n_c}$ are Lipschitz continuous with constants L_r , L_F , and L_c respectively.*

Assumption 2 (Bounded Level Sets). *For any fixed penalties (μ, γ) with $\mu \leq \mu_{\text{max}}$ and $\gamma_j \leq \gamma_{j,\text{max}}$, the level set*

$$\mathcal{L}(\mu, \gamma) = \{z : \phi_{\mu, \gamma}(z) \leq \phi_{\mu, \gamma}(z^0)\} \quad (21)$$

is compact. Furthermore, the cost residuals are bounded on this level set: $\|r_k(x_k, u_k)\| \leq R$ for all $z \in \mathcal{L}(\mu, \gamma)$ and all k .

Assumption 3 (Controlled Sampling). *At each iteration ℓ , the sampling procedure generates $\mathcal{Y}^\ell = \{y_1, \dots, y_m\}$ satisfying: (i) $y_i \in B(z^\ell, \Delta^\ell)$ for all $i \in \{1, \dots, m\}$; (ii) $z^\ell \in \mathcal{Y}^\ell$, i.e., the current iterate is included; and (iii) when $\Delta^\ell > 0$, samples provide sufficient directional coverage to detect descent directions.*

Assumption 4 (Sufficient Trust Region Contraction). *The minimum trust region radius Δ_{min} is chosen small enough such that for any trajectory z in the level set $\mathcal{L}(\mu_{\text{max}}, \gamma_{\text{max}})$, if the bundle approximation is constructed with radius Δ_{min} , then the approximation error satisfies $CL_\phi \Delta_{\text{min}} < \epsilon_{\text{feas}}$, where C is the constant from Lemma 3 and ϵ_{feas} is the convergence tolerance.*

Definition 3 (Local Stationarity). A trajectory z^* is stationary for $\phi_{\mu,\gamma}$ if for all sufficiently small $\Delta > 0$ and any sample set $\mathcal{Y} \subset B(z^*, \Delta)$ with $z^* \in \mathcal{Y}$, solving the subproblem (12) yields:

$$\lim_{\Delta \rightarrow 0} \|z^+ - z^*\| = 0, \quad (22)$$

where $z^+ = W_z \alpha^*$ is the recovered trajectory.

Remark 2. This definition captures the practical notion that no local convex combination of nearby samples improves the objective. It is the appropriate stationarity concept for derivative-free optimization [23].

Lemma 1 (Lipschitz Constant). Under Assumptions 1 and 2, the penalized objective $\phi_{\mu,\gamma}$ is Lipschitz continuous on $\mathcal{L}(\mu, \gamma)$ with constant:

$$L_\phi(\mu, \gamma) = 2HRL_r + (H-1)\mu(1+L_F+L_c) + (H-1)L_c \sum_{j=1}^J \gamma_j, \quad (23)$$

where R is the bound on cost residuals from Assumption 2.

Proof. The proof follows from standard Lipschitz composition rules; see, e.g., [23, Chapter 1]. The ℓ_1 norm and $[\cdot]_-$ operator are Lipschitz with constant 1. For the cost term, using $\|a\|^2 - \|b\|^2 = (\|a\| + \|b\|)(\|a\| - \|b\|) \leq (\|a\| + \|b\|)\|a - b\|$ and the bound $\|r_k\| \leq R$:

$$\begin{aligned} \left| \|r_k(x_k, u_k)\|^2 - \|r_k(x'_k, u'_k)\|^2 \right| &\leq 2R\|r_k(x_k, u_k) - r_k(x'_k, u'_k)\| \\ &\leq 2RL_r\|(x_k, u_k) - (x'_k, u'_k)\|. \end{aligned} \quad (24)$$

Summing over $k = 1, \dots, H$ gives the first term $2HRL_r$.

For the dynamics penalty term $\mu\|x_{k+1} - F(x_k, u_k)\|_1$:

$$\begin{aligned} &\left| \|x_{k+1} - F(x_k, u_k)\|_1 - \|x'_{k+1} - F(x'_k, u'_k)\|_1 \right| \\ &\leq \|(x_{k+1} - x'_{k+1}) - (F(x_k, u_k) - F(x'_k, u'_k))\|_1 \\ &\leq \|x_{k+1} - x'_{k+1}\|_1 + L_F\|(x_k, u_k) - (x'_k, u'_k)\|. \end{aligned} \quad (25)$$

This contributes $(1 + L_F)$ per time step. Similar analysis for constraint terms yields the stated bound. \square

Lemma 2 (Penalty Stabilization). Under Algorithm 1, there exists $K^* < \infty$ such that $\mu^\ell = \bar{\mu}$ and $\gamma_j^\ell = \bar{\gamma}_j$ for all $\ell \geq K^*$, where:

$$K^* \leq \left\lceil \log_{\rho_\mu} \left(\frac{\mu_{\max}}{\mu^0} \right) \right\rceil + \sum_{j=1}^J \left\lceil \log_{\rho_\gamma} \left(\frac{\gamma_{j,\max}}{\gamma_j^0} \right) \right\rceil. \quad (26)$$

Proof. Penalties increase geometrically by factors ρ_μ or $\rho_\gamma > 1$ in the **Adapt Penalties** step when violations exceed thresholds, and are capped at $\mu_{\max}, \gamma_{j,\max}$. Each penalty reaches its maximum after at most $\lceil \log_{\rho}(\max/\text{init}) \rceil$ increases. This finite stabilization property is standard for geometrically increasing penalty sequences; cf. [31, Section 17.2]. \square

Lemma 3 (Bundle Approximation Accuracy). Let $z^+ = W_z \alpha^*$ be the recovered trajectory from subproblem (12). Under Assumptions 1–3, the subproblem objective approximates the penalized objective with error:

$$|\phi_{\mu^\ell, \gamma^\ell}(z^+) - J_{\text{sub}}(\alpha^*, s^*, w^*, \{d_j^*\})| \leq CL_\phi \Delta^\ell, \quad (27)$$

for some constant $C > 0$ depending only on problem dimensions, where J_{sub} denotes the subproblem objective.

Proof. This bound follows from standard interpolation error analysis in derivative-free optimization [23, Chapter 10]. The subproblem approximates the cost via $\sum_k \|W_r^{(k)} \alpha^{(k)}\|^2 \approx \sum_k \|r_k(x_k^+, u_k^+)\|^2$ with interpolation error $O(\Delta^\ell)$ by Lipschitz continuity. Slack variables bound exact violations: $\|x_{k+1}^+ - F(x_k^+, u_k^+)\| \leq \|s_k^*\| + O(\Delta^\ell)$ since $W_f^{(k)} \alpha^{(k)}$ approximates $F(x_k^+, u_k^+)$ with error $O(\Delta^\ell)$. Combining these approximations yields the stated bound. \square

Lemma 4 (Descent Property). At each iteration ℓ , the algorithm satisfies:

$$\phi_{\mu^\ell, \gamma^\ell}(z^{\ell+1}) \leq \phi_{\mu^\ell, \gamma^\ell}(z^\ell) + CL_\phi \Delta^\ell. \quad (28)$$

Proof. The bounded increase property follows from the subproblem including the current iterate as a feasible point, a standard technique in trust region methods [30]. Since $z^\ell \in \mathcal{Y}^\ell$ (Assumption 3(ii)), we can represent it with weights $\alpha_i = 1$ for the index where $y_i = z^\ell$ and $\alpha_j = 0$ otherwise. For this choice of α , the dynamics constraint in (12) requires slack $s_k = F(x_k^\ell, u_k^\ell) - x_{k+1}^\ell$, which equals the dynamics defect of the current iterate. Similarly, w_k and $d_{k,j}$ equal the constraint violations of z^ℓ . Thus, the subproblem objective at this feasible point equals:

$$J_{\text{sub}}(\alpha^\ell, s^\ell, w^\ell, \{d_j^\ell\}) = \phi_{\mu^\ell, \gamma^\ell}(z^\ell) + O(\Delta^\ell), \quad (29)$$

where the $O(\Delta^\ell)$ term accounts for bundle interpolation error (Lemma 3).

Since the subproblem minimizes over all $\alpha \in \Delta^{m-1}$ and associated slacks:

$$\begin{aligned} J_{\text{sub}}(\alpha^*, s^*, w^*, \{d_j^*\}) &\leq J_{\text{sub}}(\alpha^\ell, s^\ell, w^\ell, \{d_j^\ell\}) \\ &\leq \phi_{\mu^\ell, \gamma^\ell}(z^\ell) + O(\Delta^\ell). \end{aligned} \quad (30)$$

By Lemma 3, $\phi_{\mu^\ell, \gamma^\ell}(z^{\ell+1}) \leq J_{\text{sub}}(\alpha^*, s^*, w^*, \{d_j^*\}) + CL_\phi \Delta^\ell$, which yields the result. \square

Lemma 5 (Feasibility Improvement). Suppose $\ell \geq K^*$ (penalties have stabilized at $\bar{\mu}, \bar{\gamma}$) and either $\nu_{\text{dyn}}^\ell > \tau_{\text{viol}}$ or $\nu_{\text{hard}}^\ell > \tau_{\text{viol}}$. Then the penalized objective satisfies:

$$\phi_{\bar{\mu}, \bar{\gamma}}(z^{\ell+1}) < \phi_{\bar{\mu}, \bar{\gamma}}(z^\ell), \quad (31)$$

provided the trust region Δ^ℓ is small enough that the approximation error $CL_\phi \Delta^\ell < \bar{\mu} \tau_{\text{viol}}$.

Proof. This feasibility improvement property is classical for exact penalty methods; see [31, Theorem 17.3]. When violations exceed τ_{viol} , the trust region contracts via (17), forcing samples closer to the current iterate. The subproblem finds a trajectory $z^{\ell+1}$ that reduces violations while maintaining or improving cost, since the ℓ_1 penalty terms in (12) drive the optimizer to reduce $\|s_k\|_1$ and $\|w_k\|_1$.

Since the current iterate z^ℓ is feasible for the subproblem (Lemma 4), and the subproblem minimizes, we have:

$$J_{\text{sub}}(\alpha^*, s^*, w^*, \{d_j^*\}) \leq J_{\text{sub}}(\alpha^\ell, s^\ell, w^\ell, \{d_j^\ell\}). \quad (32)$$

When $\nu_{\text{dyn}}^\ell > \tau_{\text{viol}}$ or $\nu_{\text{hard}}^\ell > \tau_{\text{viol}}$, the penalty contribution from violations is at least $\bar{\mu} \tau_{\text{viol}}$. The subproblem actively

minimizes this term, guaranteeing a reduction of at least $\bar{\mu}\tau_{\text{viol}} - CL_{\phi}\Delta^{\ell} > 0$ in the true penalized objective when $CL_{\phi}\Delta^{\ell} < \bar{\mu}\tau_{\text{viol}}$. \square

Lemma 6 (Trust Region Contraction Effect). *Under Assumption 4, when $\Delta^{\ell} = \Delta_{\min}$, the subproblem slacks satisfy:*

$$\|s_k^*\|_{\infty} < \tau_{\text{feas}}, \quad \|w_k^*\|_{\infty} < \tau_{\text{feas}}, \quad \text{for all } k, \quad (33)$$

provided z^{ℓ} is in the level set $\mathcal{L}(\mu_{\max}, \gamma_{\max})$.

Proof. The argument follows the classical trust region strategy that sufficiently small trust regions yield accurate models [30, Chapter 6]. When $\Delta^{\ell} = \Delta_{\min}$, all samples including z^{ℓ} lie within a ball of radius Δ_{\min} where the bundle approximation has error $O(\Delta_{\min})$. The subproblem's ℓ_1 penalty terms actively minimize slack variables. Since the optimizer can choose any convex combination of samples, and by Assumption 4 the approximation error satisfies $CL_{\phi}\Delta_{\min} < \epsilon_{\text{feas}} < \tau_{\text{feas}}$, the optimal slacks satisfy $\|s_k^*\|_{\infty} \leq CL_{\phi}\Delta_{\min} < \tau_{\text{feas}}$ and similarly $\|w_k^*\|_{\infty} < \tau_{\text{feas}}$. \square

Remark 3 (Violation Metric Design). *Definition 1 uses different norms for different constraint types: ν_{dyn}^{ℓ} and ν_{hard}^{ℓ} take the maximum over time of the $\|\cdot\|_{\infty}$ norm (worst-case violation at any time step), while ν_j^{ℓ} uses $\sum_k \|\cdot\|_1$ (cumulative violation). This asymmetry reflects the design philosophy that dynamics and hard constraints (state/input bounds) must be satisfied uniformly at every time step, whereas soft constraints may tolerate occasional small violations provided the cumulative violation remains bounded. Consequently, thresholds τ_{viol} and τ_j should be calibrated with this distinction in mind.*

Theorem 1 (Convergence to Feasible Stationary Points). *Under Assumptions 1–4, suppose the penalty bounds satisfy μ_{\max} and $\gamma_{j,\max}$ large enough such that the exact penalty equivalence holds (i.e., constrained stationary points are also stationary for the penalized problem when $\mu \geq \mu_{\max}$ and $\gamma_j \geq \gamma_{j,\max}$). Then Algorithm 1 satisfies:*

- (i) **Penalty Stabilization:** *There exists $K^* < \infty$ such that $(\mu^{\ell}, \gamma^{\ell}) = (\bar{\mu}, \bar{\gamma})$ for all $\ell \geq K^*$.*
- (ii) **Feasibility Attainment:** $\lim_{\ell \rightarrow \infty} (\nu_{\text{dyn}}^{\ell} + \nu_{\text{hard}}^{\ell}) = 0$.
- (iii) **Trajectory Convergence:** $\lim_{\ell \rightarrow \infty} \|z^{\ell+1} - z^{\ell}\| = 0$.
- (iv) **Stationarity:** *Every accumulation point of $\{z^{\ell}\}$ is stationary for $\phi_{\bar{\mu}, \bar{\gamma}}$ in the sense of Definition 3, and hence is a stationary point of the original constrained R2R control problem.*

Proof. **Part (i):** Immediate from Lemma 2.

Part (ii): For $\ell \geq K^*$, denote $\bar{\phi} = \phi_{\bar{\mu}, \bar{\gamma}}$. Suppose violations remain above τ_{viol} infinitely often. Each time $\nu_{\text{dyn}}^{\ell} > \tau_{\text{viol}}$ or $\nu_{\text{hard}}^{\ell} > \tau_{\text{viol}}$, the trust region contracts via (17). After at most $\lceil \log_{\beta_{\text{con}}} (\Delta_{\min}/\Delta^0) \rceil$ contractions, $\Delta^{\ell} = \Delta_{\min}$.

Once $\Delta^{\ell} = \Delta_{\min}$, Lemma 6 (using Assumption 4) ensures that subproblem slacks satisfy $\|s_k^*\|_{\infty} < \tau_{\text{feas}} < \tau_{\text{viol}}$ and $\|w_k^*\|_{\infty} < \tau_{\text{feas}} < \tau_{\text{viol}}$. This contradicts the assumption that violations remain above τ_{viol} .

Therefore, after finitely many iterations, violations drop below τ_{viol} and remain there. Once violations are below τ_{viol} , Lemma 4 ensures the penalized objective $\bar{\phi}$ is non-increasing (up to $O(\Delta^{\ell})$ error). Since $\bar{\phi}$ includes penalty

terms $\bar{\mu} \sum_k (\|s_k\|_1 + \|w_k\|_1)$, and $\bar{\phi}$ is bounded below on the compact level set (Assumption 2), the sequence $\sum_k (\|s_k\|_1 + \|w_k\|_1)$ must converge to zero, implying $\nu_{\text{dyn}}^{\ell} \rightarrow 0$ and $\nu_{\text{hard}}^{\ell} \rightarrow 0$.

Part (iii): We show trajectory convergence by contradiction. Let $\bar{\phi}^* = \liminf_{\ell \rightarrow \infty} \bar{\phi}(z^{\ell})$, which exists since $\bar{\phi}$ is bounded below on the compact level set (Assumption 2).

Suppose $\|z^{\ell+1} - z^{\ell}\| \not\rightarrow 0$. Then there exists $\delta > 0$ and a subsequence $\{k\}$ such that $\|z^{\ell_k+1} - z^{\ell_k}\| \geq \delta$ for all k .

At each such iteration, the subproblem found a solution z^{ℓ_k+1} significantly different from z^{ℓ_k} . By Assumption 3(iii), if a direction of improvement exists within radius Δ^{ℓ_k} , the sampling provides sufficient coverage to detect it. The fact that the optimizer chose z^{ℓ_k+1} with $\|z^{\ell_k+1} - z^{\ell_k}\| \geq \delta$ implies a reduction in the subproblem objective. This reduction can come from either the quadratic cost term or the penalty terms (constraint violations).

Once violations are below τ_{feas} (Part (ii)), the trust region stabilizes or expands. With bounded $\Delta^{\ell} \leq \Delta_{\max}$, the approximation errors are uniformly bounded: $CL_{\phi}\Delta^{\ell} \leq CL_{\phi}\Delta_{\max}$.

For the penalized objective, combining Lemma 3 with the subproblem optimality:

$$\begin{aligned} \bar{\phi}(z^{\ell_k+1}) &\leq J_{\text{sub}}(\alpha^*, s^*, w^*, \{d_j^*\}) + CL_{\phi}\Delta^{\ell_k} \\ &\leq \bar{\phi}(z^{\ell_k}) + 2CL_{\phi}\Delta_{\max}. \end{aligned} \quad (34)$$

Since $\bar{\phi}$ is bounded below and the sequence $\{\bar{\phi}(z^{\ell})\}$ cannot decrease by more than $O(\Delta_{\max})$ infinitely often while maintaining $\|z^{\ell+1} - z^{\ell}\| \geq \delta$, we reach a contradiction. The penalized objective would eventually need to decrease below its infimum, which is impossible. Therefore, $\|z^{\ell+1} - z^{\ell}\| \rightarrow 0$.

Part (iv): By compactness (Assumption 2), $\{z^{\ell}\}_{\ell \geq K^*}$ has accumulation points. Consider any accumulation point z^* along a subsequence $z^{\ell_k} \rightarrow z^*$. By Part (iii), $z^{\ell_k+1} \rightarrow z^*$ as well.

For any $\delta > 0$, eventually $\|z^{\ell_k} - z^*\| < \delta/2$. Consider two cases.

Case 1: Trust region bounded away from zero. If $\Delta^{\ell_k} \geq \delta' > 0$ for some δ' , then samples $\mathcal{Y}^{\ell_k} \subset B(z^*, \delta)$ provide directional coverage (Assumption 3(iii)). Along the subsequence, $\|z^{\ell_k+1} - z^{\ell_k}\| \rightarrow 0$, meaning the subproblem cannot find improving directions. By Definition 3, z^* is stationary for $\bar{\phi}$.

Case 2: Trust region contracted to Δ_{\min} . By Part (ii), z^{ℓ_k} achieves $\nu_{\text{dyn}}^{\ell_k} < \epsilon_{\text{feas}}$ and $\nu_{\text{hard}}^{\ell_k} < \epsilon_{\text{feas}}$, so it is nearly feasible. By Lemma 6, small perturbations within radius Δ_{\min} yield no improvement, again establishing stationarity.

In both cases, z^* is stationary for $\bar{\phi}$. By the exact penalty assumption, when $\bar{\mu} = \mu_{\max}$ and $\bar{\gamma}_j = \gamma_{j,\max}$, stationary points of $\bar{\phi}$ coincide with stationary points of the constrained problem [31, Theorem 17.3]. \square

Remark 4 (Soft Constraint Violations). *Theorem 1 proves convergence of dynamics and hard constraint violations to zero, but makes no claim about soft constraint violations ν_j^{ℓ} . This is intentional: soft constraints are penalized but may remain violated at the optimal trade-off between cost minimization and constraint satisfaction. Similarly, Algorithm 1 checks convergence only for dynamics and hard constraints. If*

exact soft constraint satisfaction is required, the corresponding $\gamma_{j,\max}$ should be set large enough to ensure violations are driven to zero, or the constraint should be reclassified as hard.

Remark 5 (Comparison to Classical Results). *Theorem 1 provides convergence guarantees analogous to classical trust region methods [30], but achieves them through adaptive penalty growth and trust region management based on constraint violations rather than acceptance ratios. This simplification maintains theoretical guarantees while improving computational efficiency.*

Corollary 1 (Finite-Time Feasibility). *Under the conditions of Theorem 1, Algorithm 1 achieves $\nu_{\text{dyn}}^\ell < \epsilon_{\text{feas}}$ and $\nu_{\text{hard}}^\ell < \epsilon_{\text{feas}}$ after finitely many iterations. Specifically, feasibility is achieved within:*

$$K_{\text{feas}} \leq K^* + K_\Delta \quad (35)$$

iterations, where $K^* \leq \lceil \log_{\rho_\mu}(\mu_{\max}/\mu^0) \rceil + \sum_{j=1}^J \lceil \log_{\rho_\gamma}(\gamma_{j,\max}/\gamma_j^0) \rceil$ bounds penalty stabilization and $K_\Delta = \lceil \log_{\beta_{\text{con}}}(\Delta_{\min}/\Delta^0) \rceil$ bounds trust region contractions.

Proof. Part (i) of Theorem 1 shows penalties stabilize within K^* iterations. Part (ii) shows that violations drop below τ_{viol} after at most K_Δ additional trust region contractions. Once $\Delta^\ell = \Delta_{\min}$, Lemma 6 ensures violations are below τ_{feas} , and the algorithm terminates when they fall below $\epsilon_{\text{feas}} < \tau_{\text{feas}}$. \square

V. SIMULATION RESULTS

A. Simulation Setup

The proposed Adaptive TBM was evaluated on a simulated roll-to-roll system with $N = 6$ motorized rollers and coupled web spans, representing a typical industrial functional film processing line.

Reference roller velocities $v_i^r(t)$ are computed from mass conservation to ensure equilibrium:

$$v_i^r(t) = \frac{EA - T_{i-1}(t)}{EA - T_i(t)} v_{i-1}^r(t), \quad v_0^r = v_0(t), \quad (36)$$

where E denotes Young's modulus, A the cross-sectional area, and $T_i(t)$ the tension setpoint for span i .

B. Implementation Details

The Adaptive TBM was implemented with prediction horizon $H = 15$ steps (0.15s). Following the formulation in

Section III, at each timestep the controller constructs bundle matrices and solves the convex subproblem (12):

$$\begin{aligned} \min_{\alpha, s, w, d^\pm} \quad & \sum_{k=1}^H \|W_r^{(k)} \alpha^{(k)}\|_2^2 + \mu \sum_{k=1}^{H-1} (\|s_k\|_1 + \|w_k\|_1) \\ & + \gamma_+ \sum_{k=1}^{H-1} \mathbf{1}^\top d_k^+ + \gamma_- \sum_{k=1}^{H-1} \mathbf{1}^\top d_k^- \\ \text{subject to} \quad & W_f^{(k)} \alpha^{(k)} = W_x^{(k+1)} \alpha^{(k+1)} + s_k, \\ & W_{c,\text{hard}}^{(k)} \alpha^{(k)} + w_k \geq 0, \\ & W_{c,+}^{(k)} \alpha^{(k)} + d_k^+ \geq 0, \\ & W_{c,-}^{(k)} \alpha^{(k)} + d_k^- \geq 0, \\ & \alpha^{(k)} \in \Delta^{m-1}, \quad k = 1, \dots, H, \end{aligned} \quad (37)$$

where the cost residual bundles $W_r^{(k)}$ encode the quadratic tracking objectives:

$$r_k(x_k, u_k) = \begin{bmatrix} Q^{1/2}(x_k - x_k^r) \\ R^{1/2}(u_k - u_k^r) \\ S^{1/2} \Delta u_k \end{bmatrix}. \quad (38)$$

The hard constraint bundles $W_{c,\text{hard}}^{(k)}$ encode state and input bounds ($x_{\min} \leq x_k \leq x_{\max}$, $u_{\min} \leq u_k \leq u_{\max}$), while soft constraint bundles $W_{c,+}^{(k)}$ and $W_{c,-}^{(k)}$ capture asymmetric tension bounds ($T_{\text{ref}} - \delta^- \leq T(x_k) \leq T_{\text{ref}} + \delta^+$). The trajectory is recovered via (13): $x_k^* = W_x^{(k)} \alpha^{(k)*}$, $u_k^* = W_u^{(k)} \alpha^{(k)*}$.

Asymmetric penalties $\gamma_+ = 100$ and $\gamma_- = 10$ prioritize over-tension avoidance (breakage risk) over under-tension (wrinkling), following the multiple penalty class extension in Remark 1. State weights $Q = \text{diag}(100I_N, 10I_N)$ emphasize tension regulation, while rate penalty $S = 0.1I$ ensures smooth actuation.

The implementation follows Algorithm 1 with three key components:

a) Bundle Generation: At each time index k , $m = 6N + 21$ samples are generated via a hybrid strategy satisfying Assumption 3. A deterministic stencil of $6N$ samples perturbs the nominal (\bar{x}_k, \bar{u}_k) by $\pm \Delta^\ell$ along each coordinate axis, ensuring sufficient directional coverage. An additional 20 stochastic samples drawn from $\mathcal{N}((\bar{x}_k, \bar{u}_k), \Sigma)$ enhance convex hull coverage. The current iterate is always included in the sample set, as required by Assumption 3(ii).

b) Convex Subproblem: The bundle matrices $(W_x^{(k)}, W_u^{(k)}, W_f^{(k)}, W_r^{(k)}, W_c^{(k)})$ are constructed via (7)–(11), transforming the nonlinear R2R control problem into the convex subproblem (37) over simplex-constrained interpolation weights $\alpha^{(k)}$. As noted in Section III, the subproblem is convex: the objective combines a convex quadratic term with convex ℓ_1 penalties, and all constraints are linear over the Cartesian product of simplices and non-negative orthants. The subproblem is solved using a standard convex optimization solver in 10–15 ms per iteration.

c) Adaptive Trust Region and Penalties: Following Definition 1, constraint violations are computed as $\nu_{\text{dyn}}^\ell = \max_k \|s_k^*\|_\infty$ and $\nu_{\text{hard}}^\ell = \max_k \|w_k^*\|_\infty$. The trust region adapts via (17) with expansion factor $\beta_{\text{exp}} = 1.5$, contraction

factor $\beta_{\text{con}} = 0.5$, feasibility threshold $\tau_{\text{feas}} = 10^{-4}$, and violation threshold $\tau_{\text{viol}} = 10^{-2}$. Penalties adapt via (18)–(19) with increase factor $\rho_{\mu} = \rho_{\gamma} = 2.0$. This enables robust handling of aggressive transients without manual tuning, as guaranteed by Theorem 1.

C. Tension Step Tracking

This test evaluates tracking of a tension step change while maintaining regulation in coupled zones. Webs 1, 2, 4, 5, and 6 hold constant references of 28, 36, 40, 24, and 32 N, respectively. Web 3 undergoes a step from 20 N to 44 N at $t = 0.5$ s, with unwinding velocity fixed at 0.01 m/s.

Fig. 2a shows the tension response. The Adaptive TBM tracks the 24 N step in Web 3 with rise time comparable to MPC while effectively rejecting coupling disturbances in downstream webs (T_4 – T_6), where MPPI-based methods exhibit sustained oscillations. Fig. 2b confirms that TBM generates smooth torque commands, avoiding the high-frequency chatter observed in MPPI responses.

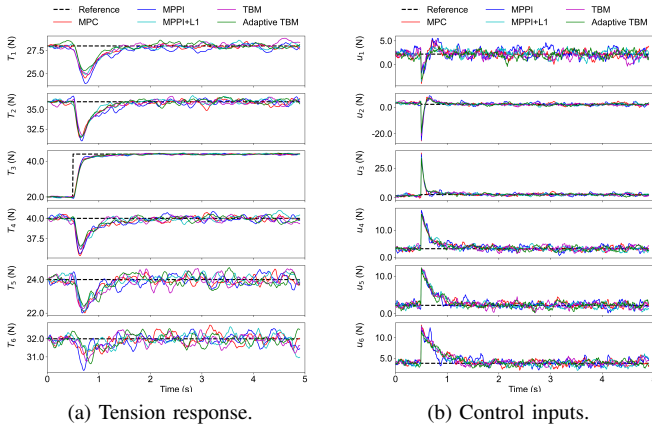


Fig. 2. Step tracking performance comparison.

D. Velocity Setpoint Change

This test evaluates tension regulation during a velocity transient. All webs maintain reference tension of 30 N while unwinding velocity increases from 0.01 m/s to 0.10 m/s at $t = 0.5$ s.

Fig. 3a shows that while all controllers experience transient tension drops due to acceleration, Adaptive TBM stabilizes downstream tensions (T_4 – T_6) faster than MPPI-based baselines. Fig. 3b confirms smooth torque generation similar to MPC.

Table I summarizes the tension RMSE across both test scenarios. Adaptive TBM achieves the lowest RMSE in both cases, outperforming gradient-based MPC by 4.3% in tension tracking and 11.1% in velocity transient regulation, while maintaining smooth actuation without derivative computation.

E. Convergence Comparison

Figure 4 compares the convergence behavior of TBM and Adaptive TBM. The adaptive variant reduces peak transient

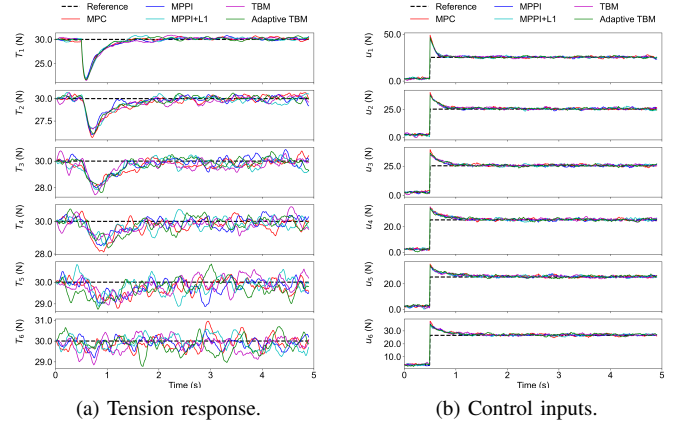


Fig. 3. Velocity change performance comparison.

TABLE I
TENSION RMSE COMPARISON (N)

| Method | Tension Step | Velocity Change |
|--------------|--------------|-----------------|
| MPC | 1.384 | 0.879 |
| MPPI | 1.419 | 0.868 |
| MPPI+L1 | 1.372 | 0.815 |
| TBM | 1.387 | 0.824 |
| Adaptive TBM | 1.324 | 0.781 |

error by 7.4% (3.15 N vs 3.4 N) in tension step tracking, as the trust region mechanism constrains step sizes during large disturbances. Additionally, Adaptive TBM converges approximately 50 iterations faster, benefiting from trust region expansion during refinement. Both methods achieve comparable steady-state accuracy (1.4 N and 0.8 N for the two scenarios), demonstrating that the adaptive mechanisms improve transient response without sacrificing final performance.

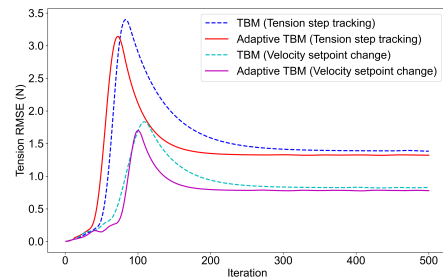


Fig. 4. Convergence comparison between TBM and Adaptive TBM.

VI. CONCLUSION

This paper developed an adaptive trajectory bundle method for R2R manufacturing control. The proposed framework combines the derivative-free simplicity of sampling-based methods with the constraint-handling rigor of sequential convex programming. Adaptive trust region and penalty mechanisms eliminate manual tuning while ensuring robust convergence. Simulation results on a six-zone R2R system demonstrate tracking accuracy comparable to gradient-based MPC and

superior disturbance rejection over MPPI baselines. The approach offers a practical solution for industrial web handling where analytical gradients are unavailable or computationally prohibitive.

ACKNOWLEDGMENTS

This should be a simple paragraph before the References to thank those individuals and institutions who have supported your work on this article.

REFERENCES

- [1] H. Koc, D. Knittel, M. De Mathelin, and G. Abba, “Modeling and robust control of winding systems for elastic webs,” *IEEE Transactions on Control Systems Technology*, vol. 10, no. 2, pp. 197–208, 2002.
- [2] P. R. Raul and P. R. Pagilla, “Design and implementation of adaptive PI control schemes for web tension control in roll-to-roll (r2r) manufacturing,” *ISA Transactions*, vol. 56, pp. 276–287, 2015.
- [3] Q. Chen, W. Li, and G. Chen, “FUZZY P+ID controller for a constant tension winch in a cable laying system,” *IEEE Transactions on Industrial Electronics*, vol. 64, no. 4, pp. 2924–2932, 2016.
- [4] C. Martin, W. Li, and D. Chen, “Stabilization of almost periodic piecewise linear systems with norm-bounded uncertainty for roll-to-roll dry transfer manufacturing processes,” in *Proceedings of the 2024 American Control Conference (ACC)*, 2024, pp. 1121–1126.
- [5] —, “Sequential quadratic programming iterative learning control for a roll-to-roll manufacturing process,” *ASME Letters in Dynamic Systems and Control*, vol. 5, no. 4, p. 041007, 2025.
- [6] J. Jeong, A. N. Gafurov, P. Park, I. Kim, H.-C. Kim, D. Kang, D. Oh, and T.-M. Lee, “Tension modeling and precise tension control of roll-to-roll system for flexible electronics,” *Flexible and Printed Electronics*, vol. 6, no. 1, p. 015005, 2021.
- [7] K. He, S. Li, P. He, J. Li, and X. Wei, “Multi-span tension control for printing systems in gravure printed electronic equipment,” *Applied Sciences*, vol. 14, no. 18, p. 8483, 2024.
- [8] C. Martin, Q. Zhao, S. Bakshi, D. Chen, and W. Li, “ h_∞ optimal control for maintaining the r2r peeling front,” *IFAC-PapersOnLine*, vol. 55, no. 37, pp. 663–668, 2022.
- [9] C. Martin, E. Kim, E. Velasquez, W. Li, and D. Chen, “ h_∞ performance analysis for almost periodic piecewise linear systems with application to roll-to-roll manufacturing control,” *arXiv preprint*, 2025.
- [10] Z. Chen, B. Qu, B. Jiang, S. R. Forrest, and J. Ni, “Robust constrained tension control for high-precision roll-to-roll processes,” *ISA Transactions*, vol. 136, pp. 651–662, 2023.
- [11] A. N. Gafurov, J. Kim, I. Kim, and T.-M. Lee, “Web tension AI modeling and reconstruction for digital twin of roll-to-roll system,” *Journal of Intelligent Manufacturing*, vol. 36, no. 7, pp. 4977–4995, 2025.
- [12] A. N. Gafurov, S. Lee, U. Ali, M. Irfan, I. Kim, and T.-M. Lee, “AI-driven digital twin for autonomous web tension control in roll-to-roll manufacturing system,” *Scientific Reports*, vol. 15, no. 1, pp. 1–17, 2025.
- [13] C. Martin, Q. Zhao, A. Patel, E. Velasquez, D. Chen, and W. Li, “A review of advanced roll-to-roll manufacturing: system modeling and control,” *Journal of Manufacturing Science and Engineering*, vol. 147, no. 4, p. 041004, 2025.
- [14] L. Park, K. Jang, and S. Kim, “Csc-mppi: A novel constrained mppi framework with dbscan for reliable obstacle avoidance,” 2025.
- [15] J. Yin, O. So, E. Yang, C. Yu, and P. Tsiotras, “Shield model predictive path integral (shield-mppi) control for robust and real-time planning,” 2023.
- [16] P. Rabiee and J. B. Hoagg, “Guaranteed-safe mppi through composite control barrier functions for efficient sampling in multi-constrained robotic systems,” 2024.
- [17] F. Wang, C. Tao, and Y. Cheng, “Mppi-dbas: Safe trajectory optimization with adaptive exploration,” 2025.
- [18] J. Borquez, L. Raus, Y. U. Ciftci, and S. Bansal, “Dualguard mppi: Safe and performant optimal control by combining sampling-based mpc and hamilton-jacobi reachability,” 2025.
- [19] O. Ezeji and et al., “Bc-mppi: A probabilistic constraint layer for safe model-predictive path-integral control,” 2025.
- [20] L. L. Yan and et al., “Output-sampled model predictive path integral control (o-mppi) for increased efficiency,” 2023.
- [21] D. M. Asmar and et al., “Control of legged robots using model predictive optimized path integral,” 2025.
- [22] K. Tracy and et al., “The trajectory bundle method: Unifying sequential-convex programming and sampling-based trajectory optimization,” 2025.
- [23] A. R. Conn, K. Scheinberg, and L. N. Vicente, *Introduction to Derivative-Free Optimization*, ser. MPS-SIAM Series on Optimization. Philadelphia: SIAM, 2009.
- [24] C. Lemaréchal, “An extension of Davidon methods to non-differentiable problems,” *Mathematical Programming Study*, vol. 3, pp. 95–109, 1975.
- [25] K. C. Kiwiel, *Methods of Descent for Nondifferentiable Optimization*, ser. Lecture Notes in Mathematics. Springer, 1985, vol. 1133.
- [26] H. G. Bock and K.-J. Plitt, “A multiple shooting algorithm for direct solution of optimal control problems,” in *Proceedings of the 9th IFAC World Congress*, 1984, pp. 243–247.
- [27] J. T. Betts, *Practical Methods for Optimal Control and Estimation Using Nonlinear Programming*, 2nd ed. SIAM, 2010.
- [28] S.-P. Han, “A globally convergent method for nonlinear programming,” *Journal of Optimization Theory and Applications*, vol. 22, pp. 297–309, 1977.
- [29] M. J. D. Powell, “A fast algorithm for nonlinearly constrained optimization calculations,” in *Numerical Analysis*, ser. Lecture Notes in Mathematics. Springer, 1978, vol. 630, pp. 144–157.
- [30] A. R. Conn, N. I. M. Gould, and P. L. Toint, *Trust-Region Methods*, ser. MPS-SIAM Series on Optimization. Philadelphia: SIAM, 2000.
- [31] J. Nocedal and S. J. Wright, *Numerical Optimization*, 2nd ed., ser. Springer Series in Operations Research. New York, NY: Springer, 2006.

VII. BIOGRAPHY SECTION

If you have an EPS/PDF photo (graphicx package needed), extra braces are needed around the contents of the optional argument to biography to prevent the LaTeX parser from getting confused when it sees the complicated `\includegraphics` command within an optional argument. (You can create your own custom macro containing the `\includegraphics` command to make things simpler here.)

If you include a photo:



Michael Shell Use `\begin{IEEEbiography}` and then for the 1st argument use `\includegraphics` to declare and link the author photo. Use the author name as the 3rd argument followed by the biography text.

If you will not include a photo:

John Doe Use `\begin{IEEEbiographynophoto}` and the author name as the argument followed by the biography text.